INVESTIGATION ON THE STRENGTH DISTRIBUTION OF UNIDIRECTIONAL CERAMIC MATRIX MINI-COMPOSITES WITH POROUS MATRIX PHASE

H. Richter*[1], M. Bartsch[1], B. Kanka[1]

[1] *Institute of Materials Research, German Aerospace Center (DLR), Linder Hoehe, 51147 Cologne, Germany*

* *Corresponding Author: henning.richter@dlr.de*

Keywords: ceramic matrix mini-composites, mechanical testing, strength distribution, statistical analysis

Abstract

In the present work, mechanical tests on unidirectional oxide/oxide ceramic matrix mini-composites with porous matrix phase were carried out. The mini-composites were manufactured by slurry infiltration and glued on mounting tabs in order to facilitate handling, alignment and clamping during mechanical testing. The specimens were thoroughly investigated by microscopy to determine their microstructural characteristics and potential surface defects.

A total of 90 specimens with different gauge lengths has been tested under uniaxial tensile loading. The test results, which were evaluated taking into account the varying fibre volume content of the specimens, demonstrate that the resulting mean tensile strength depends on gauge length.

1. Introduction

Ceramic Matrix Composites (CMCs), which consist of ceramic fibres embedded in a ceramic matrix, are aimed at overcoming the brittleness of conventional monolithic ceramics, while retaining their favourable properties, such as high-temperature stability, resistance to thermal shock and low density. Therefore, this group of materials is ideally suited to high-temperature environments, for example as burner nozzles or combustion chamber liners in industrial furnaces or gas turbines. For such applications, the CMC variant WHIPOX®, which is an acronym for Wound HIghly Porous OXide CMC, has been developed [1, 2].

WHIPOX® typically consists of alumina or mullite fibres embedded in a porous alumina or mullite matrix, however, in the following, only the alumina/alumina variant is considered. Components are fabricated via an automated filament winding process, during which the as-received continuous fibre roving is de-sized, infiltrated with water-based ceramic slurry and wound on a rotating mandrel. The green bodies are then removed from the mandrel, dried in air and sintered for one hour at a temperature of 1300 °C. As a result of the winding and sintering process, the components exhibit a laminate-like, bi-directional fibre architecture and high matrix porosity.

The non-brittle, damage tolerant behaviour of WHIPOX® tensile test specimens, which, depending on fibre orientation, manifests in a pronounced non-linearity of the stress-strain curve under mechanical loading, cf. Fig. 1, is the result of several damage mechanisms acting simultaneously on different length scales: On the laminate level (macroscale), the quasi-ductile behaviour is primarily caused by matrix shear failure, fibre re-orientation and successive rupture of fibre bundles at fibre intersections. On the fibre bundle level (mesoscale), the damage tolerant behaviour is promoted by microcrack branching, fibre-matrix debonding and by the gradual load transfer from damaged to undamaged fibres [3, 4, 5]. These damage mechanisms are enabled by a high level of matrix porosity (microscale), which assures sufficiently weak fibre-matrix bonding.

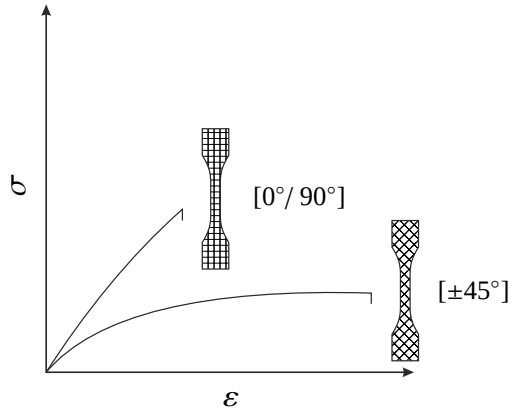

Figure 1. Typical stress-strain curves for tensile test specimens with different fibre orientations (after [4]).

From a mesoscopic point of view, the embedded reinforcement fibres can be regarded as monolithic ceramics, which exhibit size-dependent strength properties, embedded in a porous matrix of comparatively low mechanical strength. In order to study the size dependence of strength, unidirectional WHIPOX® mini-composites with three different gauge lengths were manufactured and tested under uniaxial tensile loading. Each mini-composite consists of a single fibre bundle (fibre tow), which is infiltrated with the ceramic matrix slurry and sintered at a similar temperature as standard WHIPOX® components. Therefore, the mini-composite is representative of the fibre bundles within a wound WHIPOX® component and ideally suited to investigate damage phenomena.

2. Experimental

2.1. Sample preparation and mechanical testing

The ceramic matrix mini-composites were prepared according to the standard processing route of WHIPOX® composites [1, 2]. The as-received commercial Nextel™ 610 fibre roving with 3000 den linear mass density, which corresponds to a nominal filament count of 750 [6], was passed through a furnace to burn off the organic sizing, before entering a slurry infiltration module. After infiltration with the ceramic slurry, the roving was fed through a deflector hole with an inside diameter of approximately 1 mm to remove excess slurry and to obtain a circular bundle cross-section. From the infiltrated roving, 15 sections with a length of approximately 1400 mm each were cut and placed in a drying rack to be air-dried for several hours. From each bundle section, two sets of three tensile test specimens with 50 mm, 125 mm and 250 mm

gauge length were cut, yielding a total of 30 specimens per gauge length. These specimens were sintered in air for one hour at a temperature of 1300 °C.

After sintering, the total mass and the overall length of each specimen were recorded. On one specimen from each of the 15 bundle sections, density measurements using Archimedes' principle were performed. The resulting density was assumed to be representative for all specimens cut from the respective bundle section. With the known mass and length, the volume and the average cross-sectional area of each specimen were computed.

For convenient handling and clamping, the specimens were then glued on 2 mm thick aluminium mounting tabs using a two-part epoxy adhesive, as illustrated in Fig. 2. Proper alignment of the specimens was achieved by using printed distance marks.

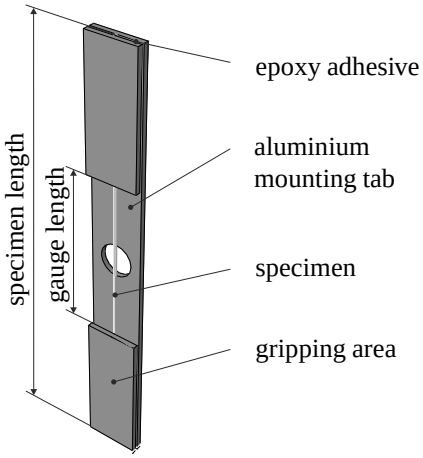

Figure 2. Mounting tab geometry used for the tensile testing of unidirectional CMC mini-composites.

Monotonic tensile tests were then carried out according to ASTM standards C1275-10 and C1557-03 [7, 8] on a dual-column Instron 5566A testing machine equipped with a 500 N load cell in a temperature and humidity controlled environment.

2.2. Microscopic investigations

Each tested specimen was investigated by optical microscopy in order to identify surface defects that may have caused premature failure. Such specimens, as well as specimens that did not fracture within gauge length, were discarded from the subsequent strength evaluation. Additionally, from each of the 15 bundle sections, a polished cross-section was prepared to determine the actual number of individual filaments within the specimens.

3. Results and discussion

3.1. Bundle microstructure

Exemplary microscopic images of two fibre bundle cross-sections are shown in Fig. 3(a). Fibre counts were between 633 and 748, and fibre volume contents ranged from 12.8 % to 44.1 %. This large variation is due to feeding the infiltrated roving through the deflector hole during

preparation of the bundle sections, which caused filament breaks. However, the number of fibres along the gauge length of each specimen can be reasonably well assumed to be constant.

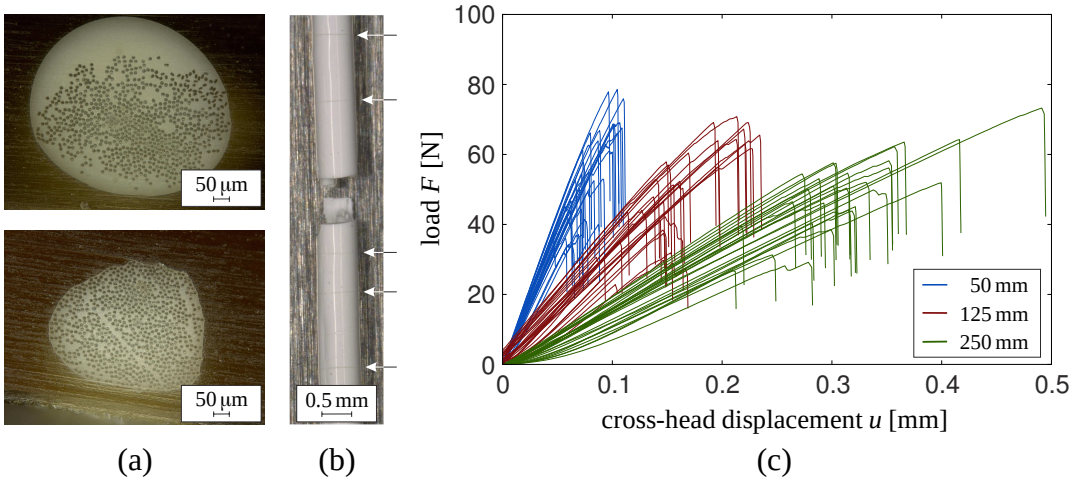

Figure 3. (a) Cross-sectional images of test specimens with a fibre volume content of 22.3 % (top) and 44.1 % (bottom), (b) multiple matrix cracks within tested fibre bundle specimen, (c) load-displacement curves of specimens with different gauge lengths.

Due to the comparatively low strength of the porous matrix, multiple matrix cracks formed readily at low loads [9, 10]. Positions of such cracks within one of the tested specimens are indicated by arrows in Fig. 3(b).

3.2. Strength distribution

The load-displacement curves of the tested fibre bundle specimens are plotted in Fig. 3(c). The measured loads at failure $F_{\max_i}$ exhibit pronounced scatter, even for specimens with the same gauge length. Due to the variation in cross-sectional area and fibre volume content, the ultimate tensile strength σ_f of each specimen was consequently determined for the effective cross-sectional area of the n fibres,

$$\sigma_\mathrm{f} = \frac{F_\mathrm{max}}{n \cdot \pi r_\mathrm{fibre}^2}, \tag{1}$$

where r_fibre denotes one half of the average fibre diameter of 11.8 µm [11]. This approach is consistent with the fact that the porous matrix fractures at low loads, and that load is carried entirely by the fibres at failure [12].

With the computed ultimate tensile strength σ_f, the probability of failure P_f of the fibre bundles can be found from the relation

$$P_\mathrm{f}(\sigma_{\mathrm{f}_i}) = \frac{i - 0.5}{N}, \tag{2}$$

where i represents the ith datum of the ranked tensile strengths and N is the actual number of

tested specimens [13]. The resulting plots of cumulative probability of failure versus tensile strength for specimens with a gauge length of 50 mm as well as 250 mm are shown in Fig. 4(a).

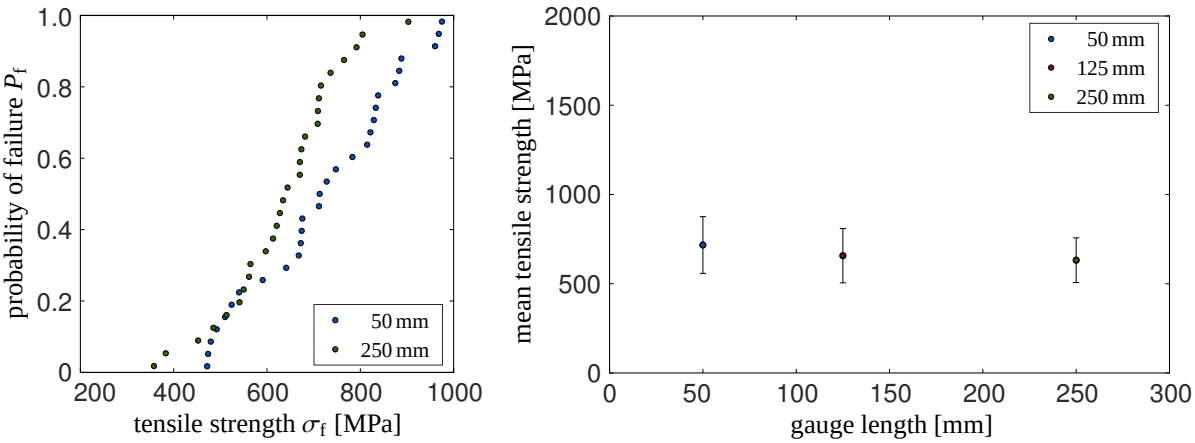

(a) (b)

Figure 4. (a) Probability of failure versus tensile strength for specimens with different gauge lengths, (b) gauge length dependence of mean tensile strength.

In Fig. 4(b), the mean tensile strength of the tested specimens is plotted as a function of gauge length. The mean tensile strength tends to decrease with increasing gauge length, which is associated with an increase of the probability of finding a flaw of critical size in a larger stressed volume.

4. Conclusions

Tensile tests on unidirectional ceramic matrix mini-composites with porous matrix phase and different gauge lengths were performed. The obtained load-displacement curves show that the specimens exhibit approximately linearly elastic behaviour up to failure, indicating that the porous matrix fractures at comparatively low loads and that load is carried evenly by the fibres after the matrix tensile strength has been exceeded. Consequently, the strength of the specimens is governed by the size-dependent strength properties of the monolithic ceramic fibres.

In order to compute the ultimate tensile strength of the specimens from the measured load at failure, the effective cross-sectional area of the fibres within each specimen has therefore to be considered. The resulting mean tensile strength exhibits a dependence on gauge length, with values decreasing from approximately 720 MPa for 50 mm gauge length to 630 MPa for 250 mm gauge length.

5. Acknowledgements

This work was funded by EU and the German Federal State of North Rhine-Westphalia. Support during specimen preparation and tensile testing was kindly provided by F. Flucht, P. W. M. Peters, U. Fuchs and M. Rakotomahefa at German Aerospace Center (DLR).

References

[1] M. Schmücker and H. Schneider. Whipox all oxide ceramic matrix composites. In N. P. Bansal, editor, *Handbook of Ceramic Composites*, pages 423–435. Springer, New York, 2005.

[2] M. Schmücker and P. Mechnich. All-oxide ceramic matrix composites with porous matrices. In W. Krenkel, editor, *Ceramic Matrix Composites: Fiber Reinforced Ceramics and their Applications*, pages 205–229. Wiley-VCH, Weinheim, 2008.

[3] A. G. Evans and F. W. Zok. The physics and mechanics of fibre-reinforced brittle matrix composites. *J. Mater. Sci.*, 29(15):3857–3896, 1994.

[4] F. W. Zok and C. G. Levi. Mechanical properties of porous-matrix ceramic composites. *Adv. Eng. Mater.*, 3(1–2):15–23, 2001.

[5] K. Tushtev, J. Horvath, D. Koch, and G. Grathwohl. Deformation and failure modeling of fiber reinforced ceramics with porous matrix. *Adv. Eng. Mater.*, 6(8):664–669, 2004.

[6] 3m Corporation. *Nextel™ Ceramic Textiles Technical Notebook*. 3m Ceramic Textiles and Composites, St. Paul, MN, 2004.

[7] ASTM Standard C1275-10. *Standard Test Method for Monotonic Tensile Behavior of Continuous Fiber-Reinforced Advanced Ceramics with Solid Rectangular Cross-Section Test Specimens at Ambient Temperature*. ASTM International, West Conshohocken, PA, 2008.

[8] ASTM Standard C1557-03. *Standard Test Method for Tensile Strength and Young's Modulus of Fibers*. ASTM International, West Conshohocken, PA, 2008.

[9] J. Lamon and N. Lissart. A statistical-probabilistic approach to microstructure-structure relations in failure and damage of ceramic composites. In G.N. Frantziskonis, editor, *PROBAMAT-21st Century: Probabilities and Materials*, pages 143–160. Springer, Dordrecht, 1998.

[10] C. Chateau, L. Gélébart, M. Bornert, J. Crépin, D. Caldemaison, and C. Sauder. Modeling of damage in unidirectional ceramic matrix composites and multi-scale experimental validation on third generation sic/sic minicomposites. *J. Mech. Phys. Solids*, 63:298–319, 2014.

[11] H. Richter. Numerical modelling of a ceramic matrix composite with porous matrix phase. In *Proceedings of the 13th ONERA-DLR Aerospace Symposium*, pages 1–10. 2013.

[12] G. N. Morscher. Tensile stress rupture of SiC_f/SiC_m minicomposites with carbon and boron nitride interphases at elevated temperatures in air. *J. Am. Ceram. Soc.*, 80(8):2029–2042, 1997.

[13] ASTM Standard C1239-07. *Standard Practice for Reporting Uniaxial Strength Data and Estimating Weibull Distribution Parameters for Advanced Ceramics*. ASTM International, West Conshohocken, PA, 2007.